Sensitivity of large-scale vegetation greenup and dormancy dates to climate change in the north-south transect of eastern China

Z. Yu [a] , P. Sun [b] , S. Liu [c] , J. Wang [a] & A. Everman [a]

[a] Division of Forestry and Natural Resources , West Virginia University , Morgantown 26506 , VA , USA

[b] Institute of Forest Ecology, Environment and Protection, Chinese Academy of Forestry , Beijing , 100091 , PR China

[c] Chinese Academy of Forestry , Beijing , PR China
Published online: 25 Jul 2013.

PLEASE SCROLL DOWN FOR ARTICLE

Taylor & Francis
Taylor & Francis Group

Sensitivity of large-scale vegetation greenup and dormancy dates to climate change in the north−south transect of eastern China

Z. Yu[a], P. Sun[b]*, S. Liu[c], J. Wang[a], and A. Everman[a]

[a]*Division of Forestry and Natural Resources, West Virginia University, Morgantown 26506, VA, USA;* [b]*Institute of Forest Ecology, Environment and Protection, Chinese Academy of Forestry, Beijing 100091, PR China;* [c]*Chinese Academy of Forestry, Beijing, PR China*

Phenology event responses, based on vegetation types, are strong indicators of climate variability and the ability of the vegetation to adapt to future climate changes. However, the sensitivity of phenology events to climate change along either environmental or vegetation type gradients is rarely examined. Phenological curves of major vegetation types along the North−South Transect of Eastern China (NSTEC) have been developed using wavelet and smooth-spline methods based on the normalized difference vegetation index from 1982 to 2006. Spatial−temporal patterns, trends of greenup-onset dates, dormancy dates, and growing season lengths (GSLs) during the period of 1982−2006 are presented.

The greenup-onset dates were most significantly and negatively related to the temperature in cold and humid areas, but insignificantly and positively in semi-arid regions. However, dormancy date showed a positive correlation with temperature. In populations of the same vegetation type, distributed along thermal gradients of NSTEC, the phenology sensitivities to warming were different. Greenup sensitivities of cold temperate coniferous forest (CTCF) and temperate meadow steppe (TMS) increased significantly from −6.0 to 0 days $°C^{-1}$ ($p < 0.001$) and from about −2.0 to 2.0 days $°C^{-1}$ ($p < 0.001$), respectively. In contrast, temperate grass steppe (TGS) and temperate deciduous shrubland (TDS) showed a decreased trend of greenup sensitivity from 2.0 to −4.0 days $°C^{-1}$ ($p < 0.001$) and from 2.0 to −6.0 days $°C^{-1}$ ($p < 0.001$), respectively. For the dormancy date sensitivity, CTCF showed a decreasing trend from about 6.0 to 0 days $°C^{-1}$ ($p < 0.001$), and subtropical evergreen-broadleaved forest (SEBF) decreased from 5.0 to −5.0 days $°C^{-1}$ ($p < 0.05$).

1. Introduction

Phenological records are a useful proxy in the study of climate change, because the seasonal pattern of vegetation is sensitive to small variations in climate (Tan et al. 2011). Vegetation phenology is an important component of dynamic vegetation models and it reflects the dynamics of the carbon−water exchange between the land surface and the atmosphere. Shifts in plant phenology are seen as fingerprints of global warming (Jentsch et al. 2009). Phenological event variation and its response to climate change have drawn a lot of attention due to increasing temperatures in the northern hemisphere since the 1980s (Chmielewski, Muller, and Bruns 2004). Advances of spring greenup have been found in mid- and high-latitude areas (Schwartz and Reiter 2000; Defila and Clot 2001; Parmesan 2007), and also

*Corresponding author. Email: sunpsen@caf.ac.cn

in low-latitude areas (Heumann et al. 2007; Xiao et al. 2006). The changes in phenological events may have potential impacts on the net primary productivity of vegetation (Lucht et al. 2002), altering global carbon, water, and nitrogen cycles, the duration of the pollination season, and the distribution of diseases (Schwartz and Reiter 2000; White, Running, and Thornton 1999; Menzel 2000). Therefore, there is a critical need to examine the relationship between climate change and phenological reponses on a large scale.

Satellite remote sensing repeatedly monitors and characterizes phenological information on a large scale (White, Thornton, and Running 1997; White et al. 2005), which reflects the seasonal cycles of leaf functions (Botta et al. 2000). Zhang, Friedl, and Schaaf (2009) investigated the impacts of temporal resolution sampling on the sensitivity of phenology detection and showed that vegetation phenology could be precisely estimated using satellite data with temporal resolutions of 6−16 days. The normalized difference vegetation index (NDVI) time-series data set is widely used because it has an advantage in presenting vegetation information in broad spatial coverage, especially in quantifying vegetation variations at regional, continental, and global scales (Reed et al. 1994; Tucker et al. 2001; Zhou et al. 2001, 2003).

Although shifts in phenology have been reported in many studies, less attention has been paid to the impacts of continuous warming on plant species sensitivies. For example, many woody plant species require chilling to break their dormancy and respond to springtime warming (Baldocchi and Wong 2008; Luedeling, Zhang, and Girvetz 2009). If chilling is insufficient, more springtime warming is required to initiate budburst for some species (Murray, Cannell, and Smith 1989). Hence, for the population of vegetation distributed in different temperature conditions, the responses of phenologic sensitivies to warming may be different. In addition, although many studies have documented the shift of phenological events in Europe (Menzel and Fabian 1999; Beaubien and Freeland 2000; Menzel, Estrella, and Fabian 2001; Zhou et al. 2001) and Eastern Asia (Piao et al. 2006; Yu et al. 2003; Chen, Hu, and Yu 2005), fewer studies have been performed on modelling vegetation phenology of plants in tropical and subtropical areas, due to the challenge of removing large amounts of noise from the remote-sensing data. Therefore, simulations of precise vegetation phenologic processes will be required before our study on vegetation phenology using remote sensing can begin, especially for tropical and subtropical areas in China.

In this study, we used the National Oceanic and Atmospheric Administration (NOAA) Advanced Very High Resolution Radiometer (AVHRR) NDVI data sets and meteorological data to examine recent trends in natural plant phenologies in the North−South Transect of Eastern China (NSTEC) from 1982 to 2006. Based on water and heat gradients along the NSTEC, this study aims (1) to develop a new algorithm to remove noise, reconstruct time-series NDVI, and detect phenological events for wide geographical ranges of vegetation; (2) to quantify change patterns in vegetation phenologic events along NSTEC over the past two decades; and (3) to investigate the response of phenologic events to climate change.

2. Study area

The NSTEC ranges longitudinally from 110° E−120° E for latitudes less than 40° N, and from longitudes 118° E−128° E for latitudes greater than 40° N, covering nearly one-third of the land area of China (Peng et al. 2002). As a core project of the International Geosphere−Biosphere Programme (IGBP), the transect was established to coordinate

diverse research activities with objectives to answer scientific questions pertinent to global change (Gao, Li, and Yang 2003). Average annual precipitation and mean temperature decrease from 1800 mm and 22°C, respectively, in the warm and humid tropical south, to 500 mm and 1°C, respectively, in the cold, semi-humid north of the transect (Gao, Li, and Yang 2003). The vegetation along the transect includes cold temperate coniferous forest (CTCF), temperate coniferous forest (TCF), temperate mixed forest (TMF), temperate deciduous-broadleaved forest (TDBF), temperate deciduous shrubland (TDS), temperate meadow steppe (TMS), temperate grass steppe (TGS), temperate grassland (TG), subtropical deciduous-broadleaved forest (SDBF), subtropical and tropical coniferous forest (STCF), subtropical evergreen-broadleaved forest (SEBF), and subtropical and tropical grassland (STG) (Figure 1).

3. Data and methods

3.1. *NDVI, climate, and land-cover data*

The NDVI data set used in this study was processed by the Global Inventory Modeling and Mapping System (GIMMS) at NASA's Goddard Space Flight Center at spatial resolution of 8 km × 8 km and 15 day intervals, as described by Tucker et al. (2005). Monthly mean temperature and precipitation data were collected from 752 standard observations and interpolated to the same resolution as NDVI using Anusplin (Ver. 4.1, Australian National University, Centre for Resources and Environmental Studies, Canberra, Australia). Vegetation type and land-cover data were obtained from digitized 1:1,000,000 vegetation maps (Compiling Committee of Vegetation Maps of 1:1000, and 000 in China 2001) and raster maps (Ran, Li, and Lu 2010) of China, respectively.

3.2. *Method*

Vegetation phenologies derived from remote-sensing methods are unequal to phenology records of species levels from a ground-measured approach. The onset of growing seasons at a species level can hardly be detected from sensors on a landscape scale. However, the large-scale land-surface phenology, which refers to aggregated information from the spatial resolution of satellite sensors, can be observed from remote-sensing platforms (Tan et al. 2011). Rather than attempting to identify a vegetation-specific developmental stage, the growing season derived from remote sensing refers to the stage of great intensity in large-scale plant activities.

3.2.1. *Spatial interpolation of meteorological variables*

Monthly mean temperature and precipitation data were interpolated to the same resolution as NDVI using Anusplin. The Anusplin package, which supports transparent analysis and interpolation of noisy multi-variate data using thin plate smoothing splines (Hutchinson and Gessler 1994), is widely used in interpolating climatic factors such as temperature and precipitation. The use of Anusplin for spatial interpolation of hydrometeorological variables and its enhanced utility over other spatial interpolation approaches, including kriging, are summarized in McVicar et al. (2007). In this study, a quart-variate partial thin plate spline incorporating a bi-variate thin plate spline as a function of longitude, latitude, and constant linear dependences on elevation was used in simulating surfaces of monthly temperature and precipitation.
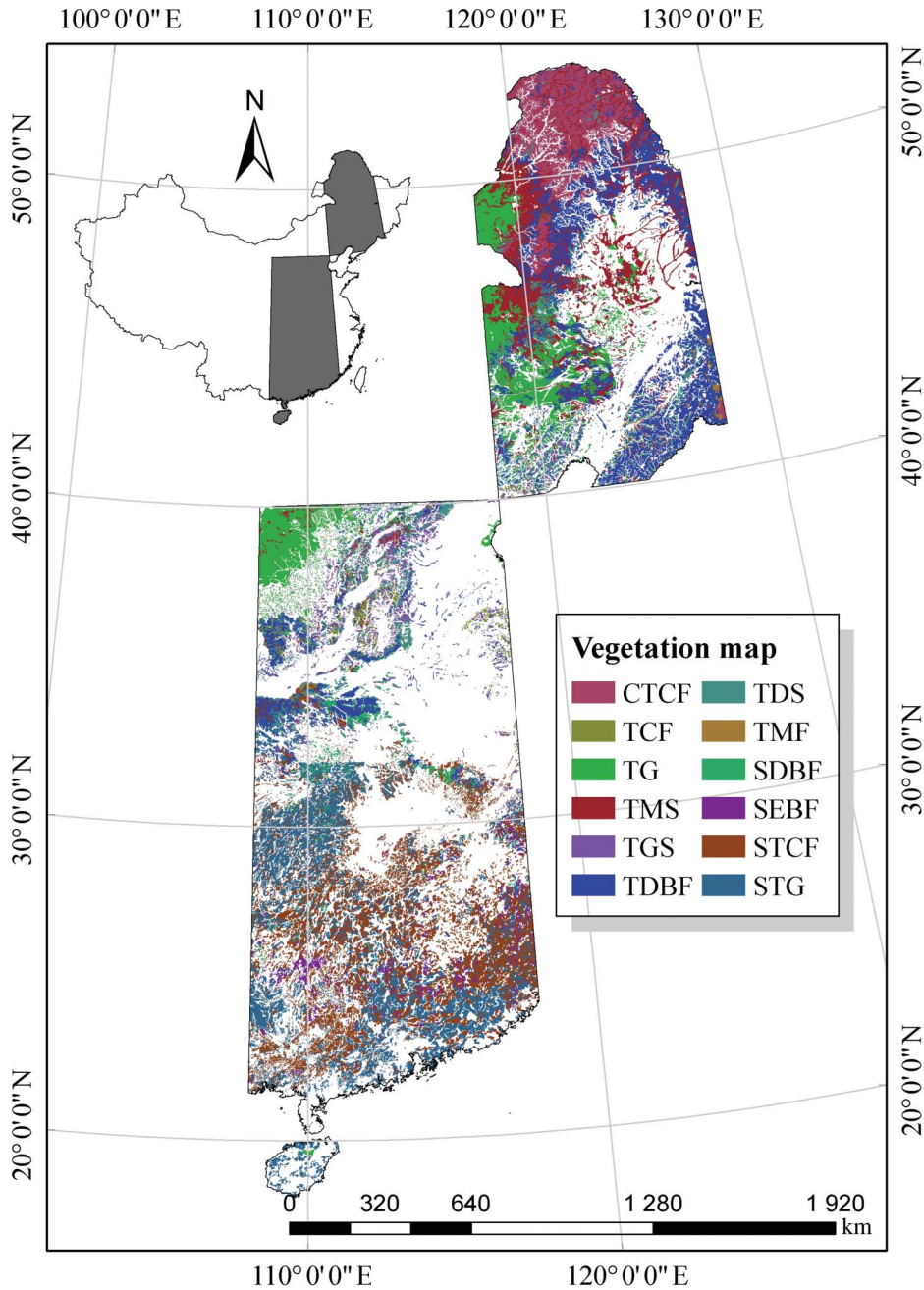
Figure 1. Vegetation types and distribution in the NSTEC.

Note: CTCF, cold temperate coniferous forest; TCF, temperate coniferous forest; TMF, temperate mixed forest; TDBF, temperate deciduous-broadleaved forest; TDS, temperate deciduous shrubland; TMS, temperate meadow steppe; TGS, temperate grass steppe; TG, temperate grassland; SDBF, subtropical deciduous-broadleaved forest; STCF, subtropical and tropical coniferous forest; SEBF, subtropical evergreen-broadleaved forest; and STG, subtropical and tropical grassland.

3.2.2. Wavelet denoising

A generalized NDVI temporal profile is continuous and smooth because vegetation canopy changes are small with respect to time (Ma et al. 2006; Bhandari, Phinn, and Gill 2011). However, there are frequent fluctuations because of the variations in cloudiness, data transmission errors, incomplete or inconsistent atmospheric corrections, and bi-directional effects in the NDVI data sets (Ma and Veroustraete 2006). Noise reduction or model fitting to raw NDVI data is therefore necessary before phenological stages can be accurately determined (Pouliot et al. 2011), especially in tropical and subtropical areas.

In this study, we employed wavelet denoising to remove the noise from raw NDVI data. Wavelets separate a signal into multi-resolution components, which are expressed by a set of functions. The set of basic functions, $\{\psi_{a,b}(t)\}$, can be generated by translating and scaling the so-called mother wavelet, $\psi(t)$, according to Daubehies (1992), and Martínez and Gilabert (2009):

$$\psi_{a,b}(t) \equiv \frac{1}{\sqrt{a}} \psi\left(\frac{t-b}{b}\right), a > 0, \; -\infty < b < \infty. \tag{1}$$

Here, the variable a is the scaling factor of a particular basis function and b is the shifting variable along the function's range (Bruce, Morgan, and Larsen 2001; Pu and Gong 2004). The function oscillates around zero and is localized in a finite-width interval (Martínez and Gilabert 2009). The smooth (low frequency) signals and the noise (high frequency) signals can be derived from wavelet decomposition. Refer to Quiroz et al. (2011) and Martínez and Gilabert (2009) for a more detailed description of the Wavelet method. The process of wavelet denoising was implemented using a multilevel 1-D wavelet decomposition package in MATLAB (v2011b, The MathWorks Inc., Natick, MA, USA).

Wavelet transformation is widely used in identifying the timing of events for a data series such as localized objective signals in the presence of noise. A few examples of these events are noise reduction in lidar signals (Fang and Huang 2004), estimating forest leaf area index (LAI), detecting the interannual variability of NOAA/AVHRR NDVI and its relationship with the El Niño/Southern Oscillation index (Li and Kafatos 2000; Park, Bayarsaikhan, and Kim 2012), and analysis of the variability of vegetation (Li and Kafatos 2000). However, wavelet transformation is seldom used for smoothing temporal NDVI data, and Figure 2 shows the denoised data set derived from raw NDVI data. Evidently, using wavelet denoising can help smooth these abnormal values and preserve the trends (variation of increase and decrease) and shape (width and amplitude) of the curve.

3.2.3. Reconstructing a daily NDVI dynamic curve by spline smoothing interpolation

The bi-weekly maximum value composite (MVC) NDVI data is obtained from the AVHRR, available from GIMMS. However, the phenologies of many plant species consist of a continuous and gradual change process for some plant attribute (Ma and Veroustraete 2006). Therefore, we need to develop a daily NDVI time-step series for convenience in further processing of phenologies. Here, we performed a spline fitting analysis of the relationship between the bi-weekly NDVI and the corresponding days of the year (DOY) from 1982 to 2006 for the whole study area, to represent the daily changes in NDVI as a function of DOY. The smoothing spline is constructed for the specified smoothing parameter t (Yu, Sun, and Liu 2010), and minimizes the following two terms for the solution:
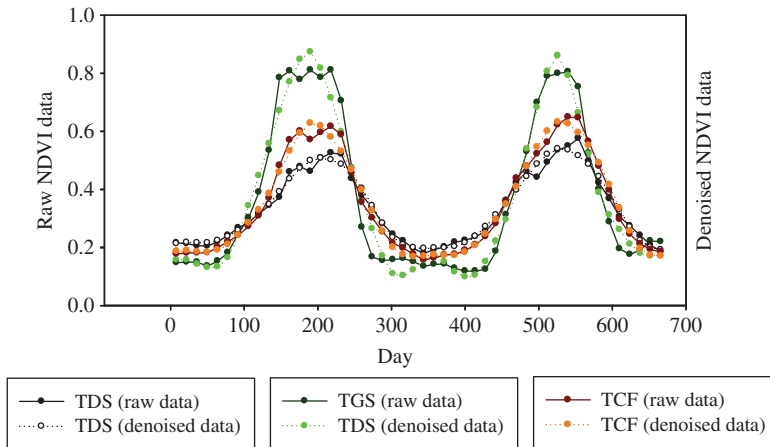
Figure 2. Wavelet denoising.

$$t \sum_i (y_i - s(x_i))^2 + (1 - t) \int \left(\frac{d^2 s}{dx^2} \right)^2 dx,$$

where *t* is defined between 0 and 1. The first term is the sum of the squares of all of the entries, which represents the deviation from input datapoints. The second term denotes the second derivative of the function, which represents the quantification of roughness of the fitted curve. As *t* moves from 0 to 1, the smoothing spline changes from a least-square straight-line fit to a cubic spline interpolant (Mathworks 2012).

The 25 year NDVI data set is deemed a continuous time series, which is advantageous in two aspects. First, since single year interpolation of previous methods can omit interannual phenologic information, the continuous time series allows for the inclusion of this data. Second, the difficulty in the identification of growing seasons in tropical and subtropical areas due to misalignment of the natural year and phenological year can be solved (Yu, Sun, and Liu 2010). Spline fit subroutines were implemented in Interactive Data Language (v4.5, the EXELIS Inc., McLean, VA, USA).

3.2.4. *Identifying vegetation phenology events*

We calculated the first and second NDVI deviations to determine the rates of change and change points in the seasonal NDVI curves. The timing of the greatest NDVI change was then used to identify the onset dates of vegetation greenup and dormancy. After phenology data were extracted, the non-vegetation pixels were masked for analysis by the land-cover map of China. In addition, the pixels of greenup dates later than 200 days and dormancy dates before 200 days were removed from the analysis because they were non-vegetation or 'contaminated' by other land-cover types. In analysing the vegetation's response sensitivities to temperature, we applied 2 km buffer zones to extract pixels in core areas of the vegetation map to further reduce noise.

3.2.5. *Sensitivity index of greenup and dormancy to temperature*

In accordance with similar studies (Han et al. 2011; Potts et al. 2008; Schwalm et al. 2010), the regression coefficients of greenup, dormancy dates, and temperature were calculated

to further explore the underlying effects of climate change on phenological variations. If phenologic events were unresponsive to temperature, then the regression coefficients are close to zero. Alternatively, if phenologic events are affected by temperature, then the regression coefficients are either positive (postponed effect) or negative (advanced effect). The greater the impacts of temperature on phenology, the larger the regression coefficients are. The slope of the linear correlation between phenologic events and temperature therefore can be applied as an easily quantifiable index of greenup and dormancy sensitivities to temperature that may be compared between sites with different acclimated temperatures.

4. Results

4.1. Distribution of phenology events

4.1.1. Greenup

The spatial patterns of greenup-onset dates generally followed the moisture gradients from east to west in northeastern China and followed the temperature gradients from the middle to the south in the transect. The earliest greenup was found in the middle of the transect (at about 100 DOY), followed by the southern region. The western portion of the northeast transect had the latest greenup date of about 150 DOY (Figure 3(*a*)). An advance in the greenup-onset date was found in most areas within the transect from 1982 to 2006. In contrast, the greenup-onset date in the northeast China plain had a positive trend (Figure 4(*a*)), suggesting that the greenup-onset dates in this area were delayed from 1982 to 2006.

4.1.2. Dormancy

The onset dates of dormancy have an evident gradient along the transect from about 300 DOY in the south to 250 DOY in the north (Figure 3(*b*)). In the past two decades, parts of the northeast region of the transect have shown a delayed trend in dormancy dates of 0−0.5 days per year (Figure 4(*b*)). In contrast, dormancy dates in the southern transect showed both advanced and delayed trends in different locations (Figure 4(*b*)).
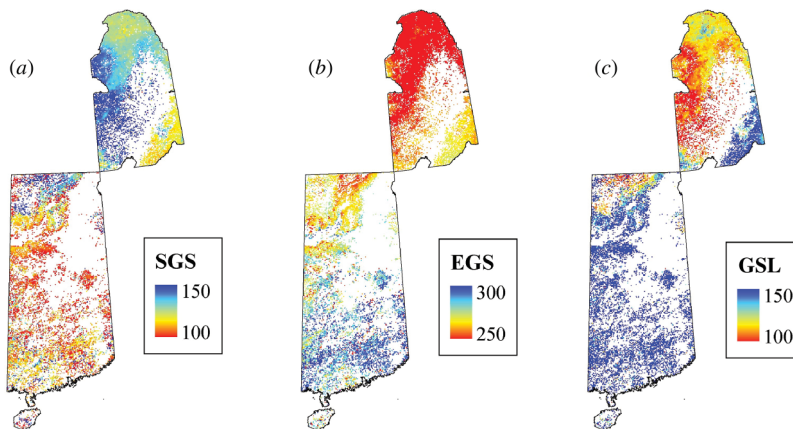

Figure 3. Distribution of (*a*) greenup date − day of year; (*b*) dormancy date − day of year; and (*c*) length of growing season − days.

Note: SGS, greenup date; EGS, dormancy date; and GSL, growing season length.
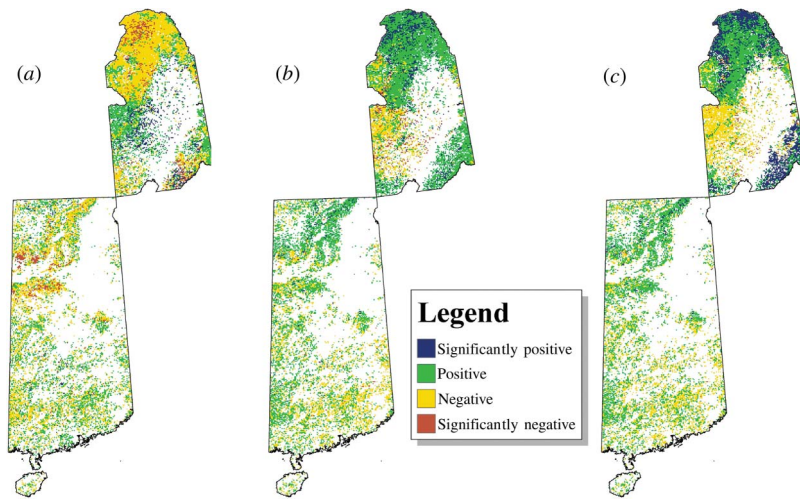
Figure 4. Distribution patterns of greenup date trend, dormancy date trend, and growing season length trend from 1982 to 2006. Blue, significantly positive at $p < 0.05$; green, insignificantly positive; yellow, insignificantly negative; and orange, significantly negative at $p < 0.05$.

4.1.3. *Growing season length*

The spatial patterns of GSLs (among different vegetation types in the NSTEC were generally linked to moisture and temperature gradients (Figure 3(*c*)). We found that the GSLs range from 100 days in the northeast to about 200 days in southwest and have lengthened from 0 to 1.0 days year^{-1} for the past two decades (Figures 3(*c*) and 4(*c*)). The lengthened trend most obviously occurred in the northernmost portion of the transect. In contrast, the western portion of the northeast showed a slightly curtailed trend of a growing season, which was distinct from other regions of the transect.

4.2. *Correlation between phenology and climatic factors*

4.2.1. *Correlation between greenup date, dormancy date, and climatic factors*

Figure 5 illustrated the spatial distribution patterns of the changing rates of mean annual temperature (MAT) and mean annual precipitation (MAP) during the period of 1982−2006. Extensive warming was detected along the NSTEC with a rate of $0.05 \pm 0.03°$C year^{-1}, with the largest amplitude increase between latitudes $36°$ N−$40°$ N (Figure 5(*a*)). MAP showed a decreasing trend in the north of the transect with a rate of 10 ± 5 mm year^{-1}, and an increasing trend in the south transect with a maximum of about 5 ± 3 mm year^{-1} (Figure 5(*b*)).

Significantly negative relationships were found between greenup dates and temperatures in the northeast and middle portions of the transect (Figure 6(*a*), $p < 0.05$). However, significantly negative correlations between greenup dates and precipitation were only found in a few locations of transect (Figure 6(*b*), $p < 0.05$). The greenup-onset dates were significantly negative when related to the temperature in cold and humid areas ($p < 0.05$), but insignificantly positive in semi-arid regions (Figure 6(*a*)). However, there is a portion in the middle of the transect, where the greenup date was significantly negatively correlated with both temperature and precipitation ($p < 0.05$), though the area is considered a semi-arid region.
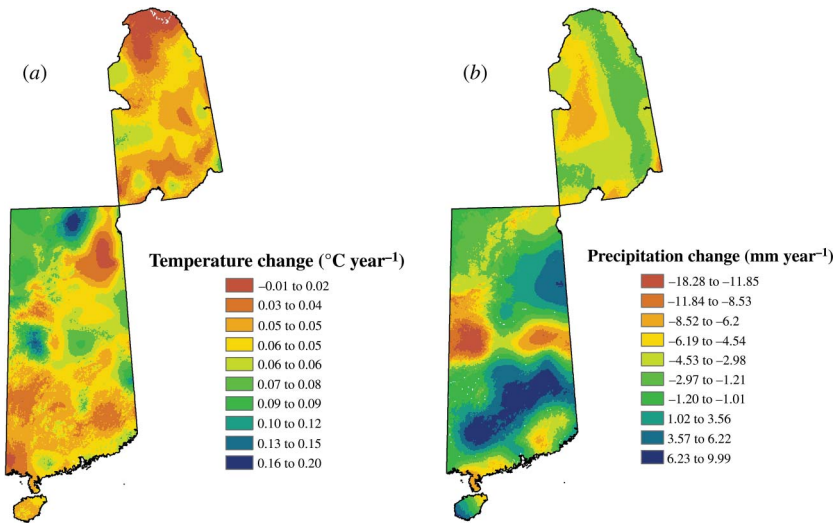
Figure 5. Distribution patterns of mean annual temperature trend (*a*) and mean annual precipitation trend (*b*).

Figure 6. Distribution patterns of correlation between greenup, temperature, and precipitation from 1982 to 2006. (*a*) greenup and temperature; (*b*) greenup and precipitation. Blue, significantly positive at $p < 0.05$; green, insignificantly positive; yellow, insignificantly negative; and orange, significantly negative at $p < 0.05$.

Increasing temperatures encourage a delay of dormancy dates in most areas of the transect, which were most significant in the north of the transect (Figure 7(*a*), $p < 0.05$). The dormancy dates of most plants in the transect showed an insignificant relation with autumn precipitation. An exception was found in the southeast region of the northeast transect, where dormancy dates showed a slightly negative relationship with temperature, but a positive relationship with precipitation.

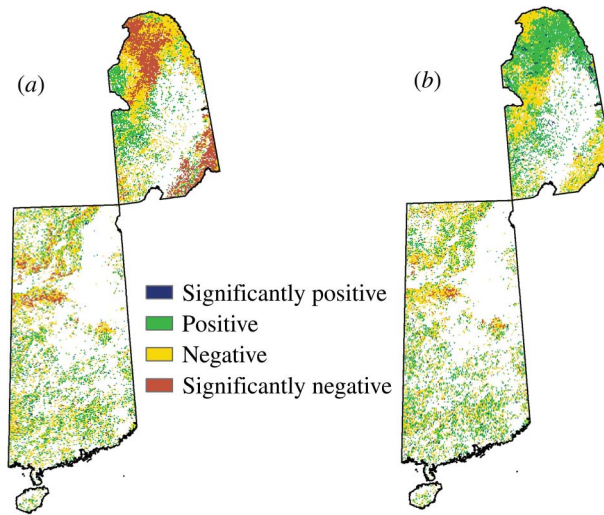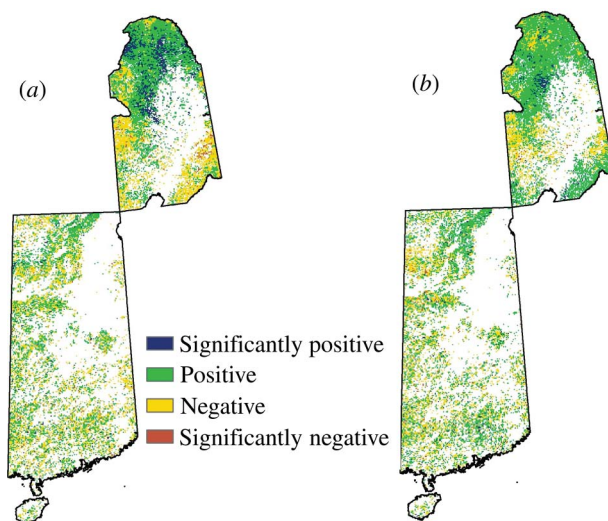Figure 7. Distribution patterns of correlation between dormancy, temperature, and precipitation from 1982 to 2006. (*a*) Dormancy and temperature; (*b*) dormancy and precipitation. Blue, significantly positive at $p < 0.05$; green, insignificantly positive; yellow, insignificantly negative; and orange, significantly negative at $p < 0.05$.

4.2.2. *Inter-vegetation phenologic sensitivities to climatic factors*

Figure 8 shows changes in different vegetation phenologies along the temperature and precipitation gradients in the NSTEC. Heat and moisture gradients along the NSTEC caused a phenological events gradient, i.e. the onset dates of greenup follow a time sequence spanning zones of cold temperate vegetation (CTCF) > temperate vegetation (TCF, TMF, TDBF, TDS, TMS, TGS, TG) > subtropical vegetation (SDBF, STCF, SEBF, STG) and the onset dates of dormancy and GSLs span zones of subtropical vegetation > temperate vegetation > cold temperate vegetation.

For different vegetation types distributed along the NSTEC, an increase of 1°C in annual temperature encourages the advancement of a greenup date by 1.54 days and the delay of dormancy date by 2.16 days, and lengthens the growing season by 3.70 days (Figure 8). In comparison, an increase of 1 mm in annual precipitation encourages the advancement of the greenup date by 0.02 days and the delay of dormancy date by 0.03 days and lengthens the growing season by 0.06 days (Figure 8). The variations in greenup dates, dormancy dates and GSLs, however, show a decreasing trend, spreading from the middle of the transect to the north and south ends.

4.2.3. *Phenologic sensitivities of vegetation acclimated under different temperatures*

We plotted the sensitivity index of each vegetation type against the acclimated temperature (average temperature of 1982 to 2006), as shown in Table 1. We found that temperature acclimation has resulted in different vegetation responses distributed along the thermal gradient of the NSTEC.

Greenup sensitivity of CTCF ranged from −6.0 to 0 days °C^{-1} with an increasing trend of 0.56 days °C^{-2} ($p < 0.001$) along the temperature gradient of the transect. Alternatively,
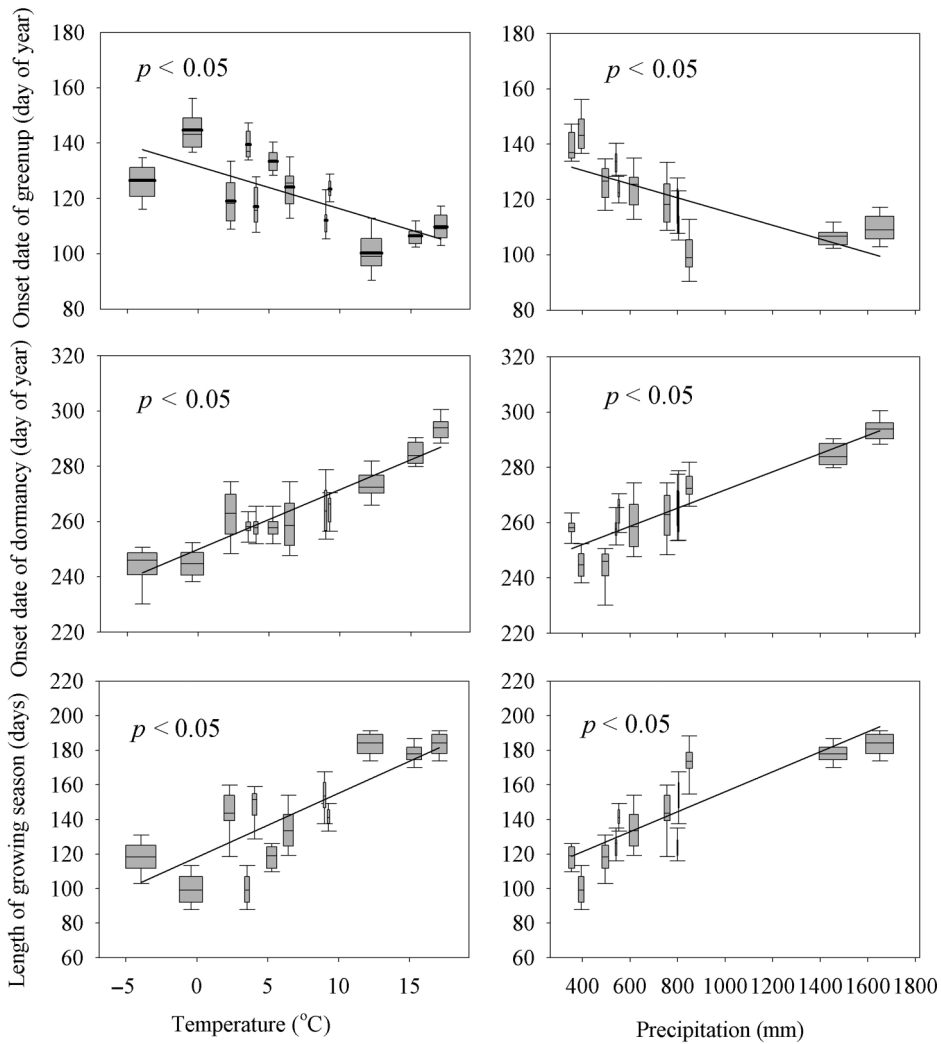
Z. Yu et al.

Figure 8. Vegetation phenology change along temperature and precipitation gradient in the NSTEC. (Along temperature gradients from low to high: CTCF, TMS, TMF, TGS, TDBF, TDS, TCF, STCF, TG, SDBF, STG, and SEBF; and along precipitation gradients from low to high: TGS, TMS, CTCF, TDS, TG, TCF, TMF, TDBF, STCF, SDBF, STG, and SEBF.)

greenup sensitivity of TDS ranges from 2.0 to -6.0 days $°C^{-1}$ with a decreasing rate of 0.07 days $°C^{-2}$ ($p = 0.001$), which means that the greenup sensitivity is greater in warm areas than in cold areas. In addition, when acclimated temperatures increase, the greenup sensitivity of TMS changes from -2.0 to 2.0 days $°C^{-1}$ with an increased rate of 0.01 days $°C^{-2}$ ($p < 0.001$); alternatively, the greenup sensitivity of TGS changes from about 2.0 to -4.0 days $°C^{-1}$ with a decreasing rate of 0.18 days $°C^{-2}$ ($p < 0.001$) from cold areas to warm areas. The dormancy sensitivity of CTCF decreases from 6.0 days $°C^{-1}$ in cold areas to 0 days $°C^{-1}$ ($p < 0.001$) in warm areas. Also, the dormancy sensitivity of SEBF changes from 5.0 days $°C^{-1}$ to -5.0 days $°C^{-1}$ with a decreasing rate of 1.15 days $°C^{-2}$ ($p < 0.05$) along the heat gradient.

Table 1. Vegetation's greenup and dormancy sensitivities to temperature.

	Greenup sensitivity			Dormancy sensitivity		
	Range (days $°C^{-1}$)	Trend (days $°C^{-2}$)	*p*-Value	Range (days $°C^{-1}$)	Trend (days $°C^{-2}$)	*p*-Value
CTCF	−6.0 to 0	0.56	< 0.001	6.0 to 0	−0.56	< 0.001
SEBF	−	−	−	5.0 to −5.0	−1.15	< 0.05
TMS	−2.0 to 2.0	0.01	< 0.001	−	−	−
TGS	2.0 to −4.0	−0.18	< 0.001	−	−	−
TDS	2.0 to −6.0	−0.07	0.001	−	−	−

5. Discussion

5.1. *Phenology variations and the impacts of climatic factors*

It is reported that many methods, such as the MVC method and the cloud algorithm for AVHRR (CLAVR), have been commonly applied on the NDVI data set to reduce error sources (Holben 1986; Stowe et al. 1991). However, significant residual effects remain in the data series (Ma and Veroustraete 2006). In this study, the Wavelet method was used to further remove noise from the raw NDVI data series, and then a spline smoothing interpolation method was performed to reconstruct a daily NDVI dynamic curve. The algorithm we presented has successfully reduced the noise, and the methods also have resolved the challenge of modelling plant phenology in tropical and subtropical areas where some methods failed to apply, such as the inverted parabola equation functional model (Piao et al. 2006). The former algorithms, which fit phenology curves for each year, lead to an omission of interannual phenology information when applied to the tropical and subtropical areas.

The earliest and latest greenup dates were found for about 100 DOY in the middle of the NSTEC and about 150 DOY in the western portion, northeast of the transect. Dormancy dates showed an evident gradient along the transect from about 300 DOY in the south to 250 DOY in the north, which is consistent with the data reported by Piao et al. (2006) in northern China. We found that NSTEC showed both an advance of greenup and a delay of dormancy at a rate of 0−1.0 days per year, and extension of the GSL at a rate of 0−2.0 days per year during the period of 1982−2006. However, the magnitude of phenology trends varied with vegetation type and location. The phenologic shift in amplitude in the NSTEC is close to that found in Europe and North America (Parmesan 2007; Stockli and Vidale 2004).

Climate variation could play a key role in interannual variability of phenology (Yu et al. 2003; Chmielewski, Muller, and Bruns 2004; Piao et al. 2006; Tao et al. 2008). Yu, Sun, and Liu (2010) reported that an extensive warming has occurred across the NSTEC during the past two decades which has contributed to the lengthening of the growing season in the northern portion, northeast of the transect. In contrast, warming and drying in arid and semi-arid regions of the NSTEC during the past two decades has resulted in a slightly curtailed trend of the GSL in the western portion of the northeast area (Figures 4(*c*) and 5). Spatial patterns of GSLs among biomes in the NSTEC have been generally linked to temperature and moisture gradients.

5.2. *Variations of phenology sensitivities of inter-vegetation types to climatic factors*

According to Thornthwaite's classification of climate of Chang (1955), the southern transect and the western portion of the northeast transect were classified as humid, arid, and

semi-arid based on the amount of water available. The relationship between greenup-onset dates and temperature were most significantly negative in cold and humid areas ($p < 0.05$), but insignificantly positive in semi-arid regions, suggesting that temperature-induced water stress could delay greenup in semi-arid areas. This conclusion was also supported by the slightly negative correlation between precipitation and greenup dates in arid and semi-arid areas (the western portion of the northeast transect), indicating that spring rainfall contributes to the mitigation of water stress in the area. Tao et al. (2008) also suggested that water stress during the preceding months could delay greenup onset in the arid and semi-arid regions of the northeast China Transect.

Dormancy dates were slightly negatively correlated with temperature but positively correlated with precipitation in the southeast portion of the northeast transect, suggesting that the dormancy of vegetation in the warm and humid areas was greatly affected by water stress. In the northern portion of the northeast transect, which is predominately cold and humid, however, vegetation dormancy was primarily controlled by heat, because warming encourages the delay of dormancy dates in the region.

5.3. *Greenup sensitivities of inter-vegetation types to climatic factors*

For the same type of vegetation, distributed in different temperature conditions, the phenologic sensitivities to warming were different. We found that trends of greenup sensitivity along the heat gradients of NSTEC varied with vegetation type.

For tree types, the greenup onset may be controlled by three key factors: the degree of winter chilling, photoperiod (day length relative to night length), and temperature (Chuine and Cour 1999; Hay 1990; Körner and Basler 2010). Insufficient chilling in the winter may delay spring bud break (Murray, Cannell, and Smith 1989; Körner and Basler 2010), which would lead to an advance in bloom dates of lilac, caused by a reduction in chilling accumulation at a rate of -1.6 to -2.2 days per 100 hours, compared with the much higher rate of -5.0 to -4.2 days per 100 hour reduction after the chilling requirement has been met (Schwartz and Hanes 2010). We also found that greenup sensitivity of CTCF ranged from -6.0 to 0 days $°C^{-1}$ with an increased rate of 0.56 days $°C^{-2}$ ($p < 0.001$) along the thermal gradient of the transect. Low greenup sensitivity of CTCF in warmer areas may be a result of reduced chilling hours in the dormancy period, because the chilling requirement was easier to attain in colder areas; this in turn encouraged higher heating units for the onset of plant growth in the spring (Chen, Hu, and Yu 2005) and led to a much lower sensitivity to warming in comparatively warm areas.

Sun et al. (2012) reported that TMS had suffered from growing season water deficits from 1982 to 2006. Changing trends in greenup sensitivity from negative to positive indicated that spring phenophases of TMS may be affected by water stresses in the area. These plants are more vulnerable to temperature-induced water stresses in warmer areas than in cooler areas, which can be seen from the conversion of greenup sensitivity from an advanced effect (negative) to a postponed effect (positive). With an increasing intensity of warming, the reduced carbon sequestration of shorter growing seasons in warmer areas may offset the increases of carbon sequestration in colder areas.

TGS and TDS are grass and shrub species distributed in areas dominated by humid and warm climates. These types of plants showed a greenup sensitivity change from positive to negative, suggesting that warming may postpone greenup dates in cold areas but will advance the greenup dates in warm areas.

5.4. *Dormancy sensitivities of inter-vegetation types to climatic factors*

Dormancy sensitivity of CTCF continued to decrease from 6.0 to 0 days $°C^{-1}$ with acclimation temperature increases from $-8.0°C$ to $0°C$ ($p < 0.001$). This indicates that warming has a larger impact on postponing dormancy dates in colder areas than in warmer areas. The dormancy dates of CTCF tend to become less sensitive to temperature with long-term warming acclimation. Therefore, the warming effect on the lengthening of the growing season of CTCF is reduced as dormancy sensitivity decreases.

In comparison, the dormancy sensitivities of SEBF change from positive to negative along the heat gradient ($p < 0.05$), indicating that warming postponed dormancy in cooler areas but advanced dormancy in warmer areas. However, dormancy sensitivities of TCF, TG, TDS, TMS, TGS, TDBF, TMF, SDBF, STG, and STCF have no significant trends under different acclimation temperatures. Dormancy dates of these vegetation types tend to have constant responses to climate change.

The sensitivities of vegetation to climate change were assumed to be constant when modelling the global carbon cycle (Kaduk and Heimann 1996). However, we found that the greenup sensitivities of CTCF, TG, TMS, TGS, and TDS and dormancy sensitivities of CTCF and SEBF will change with warming. Therefore, the global cycle models, with consideration of the change, may draw completely different results.

6. Conclusions

In our study, the wavelet and spline methods were employed to detect vegetation phenologies and analyse their responses to climatic variables. The greenup date was affected more by temperature than precipitation and was most significantly and negatively related to the temperature in humid areas, and positively and insignificantly related in semi-arid regions. In contrast, the dormancy date mainly showed a positive correlation with temperature.

The greenup sensitivity for CTCF significantly increased from negative to 0 with increasing acclimated temperatures. Also, the greenup sensitivity in TMS significantly increased from negative to positive, while the greenup sensitivities of TGS and TDS reversed from positive to negative. For dormancy, CTCF is more sensitive in cold areas than in warm areas. In comparison, dormancy sensitivities of SEBF reversed from positive to negative along the thermal gradient.

References

Baldocchi, D., and S. Wong. 2008. "Accumulated Winter Chill is Decreasing in the Fruit Growing Regions of California." *Climatic Change* 87: 153–166.

Beaubien, E. G., and H. J. Freeland. 2000. "Spring Phenology Trends in Alberta, Canada: Links to Ocean Temperature." *International Journal of Biometeorology* 44: 53–59.

Bhandari, S., S. Phinn, and T. Gill. 2011. "Assessing Viewing and Illumination Geometry Effects on the MODIS Vegetation Index (MOD13Q1) Time Series: Implications for Monitoring Phenology

and Disturbances in Forest Communities in Queensland, Australia." *International Journal of Remote Sensing* 32: 7513–7538.

Botta, A., N. Viovy, P. Ciais, P. Friedlingstein, and P. Monfray. 2000. "A Global Prognostic Scheme of Leaf Onset Using Satellite Data." *Global Change Biology* 6: 709–725.

Bruce, L. M., C. Morgan, and S. Larsen. 2001. "Automated Detection of Subpixel Hyperspectral Targets with Continuous and Discrete Wavelet." *IEEE Transactions on Geoscience and Remote Sensing* 39: 2217–2226.

Chang, T. H. 1955. "The Climate of China According to the New Thornthwaite Classification." *Annals of the Association of American Geographers* 45: 393–403.

Chen, X. Q., B. Hu, and R. Yu. 2005. "Spatial and Temporal Variation of Phenological Growing Season and Climate Change Impacts in Temperate Eastern China." *Global Change Biology* 11: 1118–1130.

Chmielewski, F. M., A. Muller, and E. Bruns. 2004. "Climate Changes and Trends in Phenology of Fruit Trees and Field Crops in Germany, 1961−2000." *Agricultural and Forest Meteorology* 121: 69–78.

Chuine, I., and P. Cour. 1999. "Climatic Determinants of Budburst Seasonality in Four Temperate-Zone Tree Species." *New Phytologist* 143: 339–349.

Compiling Committee of Vegetation Maps of 1:1,000,000 in China. 2001. *Atlas of Vegetation Maps of 1:1,000,000 in China*. Beijing: Science Press.

Daubehies, I. 1992. "CBMS-NSF Regional Conference Series in Applied Mathematics." In *Ten Lectures on Wavelets*. Philadelphia, PA: Society for Industrial and Applied Mathematics.

Defila, C., and B. Clot. 2001. "Phytophenological Trends in Switzerland." *International Journal of Biometeorology* 45: 203–207.

Fang, H. T., and D. S. Huang. 2004. "Noise Reduction in Lidar Signal Based on Discrete Wavelet Transform." *Optics Communications* 233: 67–76.

Gao, Q., X. B. Li, and X. S. Yang. 2003. "Responses of Vegetation and Primary Production in North-South Transect of Eastern China to Global Change Under Land Use Constraint." *Acta Botanica Sinica* 45: 1274–1284.

Han, W. X., J. Y. Fang, P. B. Reich, F. Ian Woodward, and Z. H. Wang. 2011. "Biogeography and Variability of Eleven Mineral Elements in Plant Leaves Across Gradients of Climate, Soil and Plant Functional Type in China." *Ecology Letter* 14: 788–796.

Hay, R. K. M. 1990. "The Influence of Photoperiod on the Dry Matter Production of Grasses and Cereals." *New Phytologist* 116: 233–254.

Heumann, B. W., J. W. Seaquist, L. Eklundh, and P. Jönsson. 2007. "AVHRR Derived Phenological Change in the Sahel and Soudan, Africa, 1982−2005." *Remote Sensing of Environment* 108: 385–392.

Holben, B. N. 1986. "Characteristics of Maximum-Value Composite Images from Temporal AVHRR Data." *International Journal of Remote Sensing* 7: 1417–1434.

Hutchinson, M. F., and P. E. Gessler. 1994. "Splines − More than Just a Smooth Interpolator." *Geoderma* 62: 45–67.

Jentsch, A., J. Kreyling, J. Boettcher-Treschkow, and C. Beierkuhnlein. 2009. "Beyond Gradual Warming: Extreme Weather Events Alter Flower Phenology of European Grassland and Heath Species." *Global Change Biology* 15: 837–849.

Kaduk, J., and M. Heimann. 1996. "A Prognostic Phenology Scheme for Global Terrestrial Carbon Cycle Models." *Climate Research* 6: 1–19.

Körner, C., and D. Basler. 2010. "Phenology Under Global Warming." *Science* 327: 1461–1462.

Li, Z. T., and M. Kafatos. 2000. "Interannual Variability of Vegetation in the United States and Its Relation to El Nino/Southern Oscillation." *Remote Sensing of Environment* 71: 239–247.

Lucht, W., I. C. Prentice, R. B. Myneni, S. Sitch, P. Friedlingstein, W. Cramer, P. Bousquet, W. Buermann, and B. Smith. 2002. "Climatic Control of the High-Latitude Vegetation Greening Trend and Pinatubo Effect." *Science* 296: 1687–1689.

Luedeling, E., M. H. Zhang, and E. H. Girvetz. 2009. "Climatic Changes Lead to Declining Winter Chill for Fruit and Nut Trees in California During 1950−2099." *PLoS One* 4: 6166.

Ma, M. G., and F. Veroustraete. 2006. "Reconstructing Pathfinder AVHRR Land NDVI Time-Series Data for the Northwest of China." *Advances in Space Research* 37: 835–840.

Martinez, B., and M. A. Gilabert. 2009. "Vegetation Dynamics from NDVI Time Series Analysis Using the Wavelet Transform." *Remote Sensing of Environment* 113: 1823–1842.

Mathworks. 2012. Curve Fitting Toolbox: Smoothing Splines. Accessed December 21, 2012. http://www.mathworks.com/help/curvefit/smoothing-splines.html

Mcvicar, T. R., T. G. Van Niel, L. T. Li, M. F. Hutchinson, X. M. Mu, and Z. H. Liu. 2007. "Spatially Distributing Monthly Reference Evapotranspiration and Pan Evaporation Considering Topographic Influences." *Journal of Hydrology* 338: 196–220.

Menzel, A. 2000. "Trends in Phenological Phases in Europe Between 1951 and 1996." *International Journal of Biometeorology* 44: 76–81.

Menzel, A., N. Estrella, and P. Fabian. 2001. "Spatial and Temporal Variability of the Phenological Seasons in Germany from 1951 to 1996." *Global Change Biology* 7: 657–666.

Menzel, A., and P. Fabian. 1999. "Growing Season Extended in Europe." *Nature* 397: 659.

Murray, M. B., M. G. R. Cannell, and R. I. Smith. 1989. "Date of Budburst of Fifteen Tree Species in Britain Following Climatic Warming." *Journal of Applied Ecology* 26: 693–700.

Park, K. A., U. Bayarsaikhan, and K. R. Kim. 2012. "Effects of El Nino on Spring Phenology of the Highest Mountain in North-East Asia." *International Journal of Remote Sensing* 33: 5268–5288.

Parmesan, C. 2007. "Influences of Species, Latitudes and Methodologies on Estimates of Phenological Response to Global Warming." *Global Change Biology* 13: 1860–1872.

Peng, S., P. Zhao, H. Ren, and F. Y. Zheng. 2002. "The Possible Heat-Driven Pattern Variation of Zonal Vegetation and Agricultural Ecosystems Along the North-South Transect of China Under the Global Change." *Earth Science Frontiers* 9: 217–226.

Piao, S. L., J. Y. Fang, L. M. Zhou, P. Ciais, and B. Zhu. 2006. "Variations in Satellite-Derived Phenology in China's Temperate Vegetation." *Global Change Biology* 12: 672–685.

Potts, D. L., R. L. Scott, J. M. Cable, T. E. Huxman, and D. G. Williams. 2008. "Sensitivity of Mesquite Shrubland CO_2 Exchange to Precipitation in Contrasting Landscape Settings." *Ecology* 89: 2900–2910.

Pouliot, D., R. Latifovic, R. Fernandes, and I. Olthof. 2011. "Evaluation of Compositing Period and AVHRR and MERIS Combination for Improvement of Spring Phenology Detection in Deciduous Forests." *International Journal of Remote Sensing* 115: 158–166.

Pu, R. L., and P. Gong. 2004. "Wavelet Transform Applied to EO-1 Hyperspectral Data for Forest LAI and Crown Closure Mapping." *Remote Sensing of Environment* 91: 212–224.

Quiroz, R., C. Yarleque, A. Posadas, V. Mares, and W. W. Immerzeel. 2011. "Improving Daily Rainfall Estimation from NDVI Using a Wavelet Transform." *Environmental Modelling and Software* 26: 201–209.

Ran, Y. H., X. Li, and L. Lu. 2010. "Evaluation of Four Remote Sensing Based Land Cover Products over China." *International Journal of Remote Sensing* 31: 391–401.

Reed, B. C., J. F. Brown, D. Vanderzee, T. R. Loveland, J. W. Merchant, and D. O. Ohlen. 1994. "Measuring Phenological Variability from Satellite Imagery." *Journal of Vegetation Science* 5: 703–714.

Schwalm, C. R., C. A. Williams, K. Schaefer, A. Arneth, D. Bonal, N. Buchmann, J. Q. Chen, B. E. Law, A. Lindroth, S. Luyssaert, M. Reichstein, and A. D. Richardson. 2010. "Assimilation Exceeds Respiration Sensitivity to Drought: A FLUXNET Synthesis." *Global Change Biology* 16: 657–670.

Schwartz, M. D., and J. M. Hanes. 2010. "Continental-Scale Phenology: Warming and Chilling." *International Journal of Climatology* 30: 1595–1598.

Schwartz, M. D., and B. E. Reiter. 2000. "Changes in North American Spring." *International Journal of Biometeorology* 20: 929–932.

Stockli, R., and P. L. Vidale. 2004. "European Plant Phenology and Climate as Seen in a 20-Year AVHRR Land-Surface Parameter Dataset." *International Journal of Remote Sensing* 25: 3303–3330.

Stowe, L. L., E. P. Mcclain, R. Carey, P. Pellegrino, G. G. Gutman, P. Davis, C. Long, and S. Hart. 1991. "Global Distribution of Cloud Cover Derived from NOAA/AVHRR Operational Satellite Data." *Advance in Space Research* 11: 51–54.

Sun, P. S., Z. Yu, S. R. Liu, X. H. Wei, J. X. Wang, and N. Zegre. 2012. "Climate Change, Growing Season Water Deficit and Vegetation Activity Along the North-South Transect of Eastern China from 1982 Through 2006." *Hydrology and Earth System Sciences Discussions* 9: 6649–6688.

Tan, B., J. T. Morisette, R. E. Wolfe, F. Gao, G. A. Ederer, J. Nightingale, and J. A. Pedelty. 2011. "An Enhanced TIMESAT Algorithm for Estimating Vegetation Phenology Metrics from MODIS Data." *IEEE Journal of Selected Topics in Applied Earth Observations and Remote Sensing* 4: 361–371.

Tao, F., M. Yokozawa, Z. Zhang, Y. Hayashi, and Y. Ishigooka. 2008. "Land Surface Phenology Dynamics and Climate Variations in the North East China Transect (NECT), 1982−2000." *International Journal of Remote Sensing* 29: 5461–5478.

Tucker, C. J., J. E. Pinzon, M. E. Brown, D. A. Slayback, E. W. Pak, R. Mahoney, E. F. Vermote, and N. El Saleous. 2005. "An Extended AVHRR 8-km NDVI Dataset Compatible with MODIS and SPOT Vegetation NDVI Data." *International Journal of Remote Sensing* 26: 4485–4498.

Tucker, C. J., D. A. Slayback, J. E. Pinzon, S. O. Los, R. B. Myneni, and M. G. Taylor. 2001. "Higher Northern Latitude Normalized Difference Vegetation Index and Growing Season Trends from 1982 to 1999." *International Journal of Biometeorology* 45: 184–190.

White, M. A., F. Hoffman, W. W. Hargrove, and R. R. Nemani. 2005. "A Global Framework for Monitoring Phenological Responses to Climate Change." *Geophysical Research Letters* 32: 1–4.

White, M. A., S. W. Running, and P. E. Thornton. 1999. "The Impact of Growing-Season Length Variability on Carbon Assimilation and Evapotranspiration over 88 Years in the Eastern US Deciduous Forest." *International Journal of Biometeorology* 42: 139–145.

White, M. A., P. E. Thornton, and S. W. Running. 1997. "A Continental Phenology Model for Monitoring Vegetation Responses to Interannual Climatic Variability." *Global Biogeochemical Cycles* 11: 217–234.

Xiao, X. M., S. Hagen, Q. Y. Zhang, M. Keller, and B. Moore. 2006. "Detecting Leaf Phenology of Seasonally Moist Tropical Forests in South America with Multi-Temporal MODIS Images." *Remote Sensing of Environment* 103: 465–473.

Yu, F., K. P. Price, J. Ellis, and P. Shi. 2003. "Response of Seasonal Vegetation Development to Climatic Variations in Eastern Central Asia." *Remote Sensing of Environment* 87: 42–54.

Yu, Z., P. S. Sun, and S. R. Liu. 2010. "Phenological Change of Main Vegetation Types Along a North-South Transect of Eastern China." *Chinese Journal of Plant Ecology* 34: 316–329.

Zhang, X. Y., M. A. Friedl, and C. B. Schaaf. 2009. "Sensitivity of Vegetation Phenology Detection to the Temporal Resolution of Satellite Data." *International Journal of Remote Sensing* 30: 2061–2074.

Zhou, L., R. K. Kaufmann, Y. Tian, R. B. Myneni, and C. J. Tucker. 2003. "Relation Between Interannual Variations in Satellite Measures of Vegetation Greenness and Climate Between 1982 and 1999." *Journal of Geophysical Research* 108: 1–11.

Zhou, L., C. J. Tucker, R. K. Kaufmann, D. Slayback, N. V. Shabanov, and R. B. Myneni. 2001. "Variations in Northern Vegetation Activity Inferred from Satellite Data of Vegetation Index During 1981−1999." *Journal of Geophysics Research* 106: 20069–20083.